

Steinkern spiders: A microbial mat-controlled taphonomic pathway in the Oligocene Aix-en-Provence Lagerstätte, France


MATTHEW R. DOWNEN^{1,*}, JAMES D. SCHIFFBAUER^{2,3}, PAUL A. SELDEN^{1,4} & ALISON N. OLCOTT¹


¹Department of Geology, University of Kansas, Lawrence, KS 66045, USA

²Department of Geological Sciences, University of Missouri, Columbia, MO 65211, USA


³X-ray Microanalysis Laboratory, University of Missouri, Columbia, MO 65211, USA

⁴Natural History Museum, Cromwell Road, London SW7 5BD, UK

✉ mattdownen@ku.edu;  <https://orcid.org/0000-0002-9837-1445>

✉ schiffbauerj@missouri.edu;  <https://orcid.org/0000-0003-4726-0355>

✉ selden@ku.edu;  <https://orcid.org/0000-0001-7454-4260>

✉ olcott@ku.edu;  <https://orcid.org/0000-0002-6854-646X>

*Corresponding author

Abstract

The Aix-en-Provence Formation is an Oligocene (22.5 Ma) Lagerstätte in southern France that contains an abundance of soft-bodied fossils preserved in exceptional detail. Many taxa have been described from this formation, including insects, spiders, fishes, and plants, suggesting a diverse ecosystem in a subtropical, brackish, lacustrine paleoenvironment. Fossil spiders from this deposit are preserved as compression fossils and internal and external molds. Recently, compression fossils of spiders from Aix-en-Provence were hypothesized to be a product of a taphonomic pathway based on diatoms and sulfurization. Here, we examine fossil spiders preserved as molds to uncover a second taphonomic pathway based on microbial mats. Evidence of microbial mats include wrinkles, pustular textures, and possible microbial mat chips on the bedding surfaces as well as a matrix fabric that contains possible microbial sheaths and bacterial spherules. The evidence presented here supports prolific microbial mat communities during deposition of the Aix-en-Provence Formation, and suggests that they are likely responsible for the moldic preservation of the spiders. Our work shows that the paleoenvironment of the Aix-en-Provence Formation promoted at least two possible taphonomic pathways that resulted in the differing modes of preservation observed.

Keywords: taphonomy, spiders, microbial mat, preservation, lacustrine

Introduction

Terrestrial arthropods, like spiders, are relatively rare in the fossil record. Most of what we know of the fossil record of spiders comes from exceptionally

preserved fossil deposits, also known as Lagerstätten, which preserve soft tissues and soft-bodied organisms (Seilacher, 1970). As these deposits can preserve remains with high fidelity, they provide a wealth of information about biodiversity and paleoecology as well as revealing morphological detail for systematic studies (Allison, 1988; Allison & Briggs, 1993; Muscente *et al.*, 2017). Understanding the taphonomic processes and pathways leading to fossilization in these deposits is crucial for informing anatomical and morphological interpretations and paleoenvironmental conditions.

In these deposits, fossil insects and spiders are often preserved as compressions, in which only a thin layer of carbonaceous material remains along with possible very low relief impressions (Martínez-Delclòs *et al.*, 2004; Gupta *et al.*, 2006). This type of preservation is observed in the Oligocene Aix-en-Provence Formation, a Lagerstätte in France. Recently, Olcott *et al.* (2022) proposed a taphonomic pathway leading to compression fossils in the Aix-en-Provence Formation based on sulfurization via diatoms and the sticky extracellular polymeric substances (EPS) they produce. The compression fossils examined were observed to be composed of a carbon-sulfur polymer and covered in dense accumulations of mat-forming pennate diatoms. The proposed taphonomic pathway for compression fossils in the Aix-en-Provence Formation involves the entrapment of a spider in the EPS of a planktonic diatomaceous mat. Chemical reactions between the chitin of the spider exoskeleton and the sulfur-rich diatom EPS begin and continue as the spider sinks through the water column. Ultimately, organic material in the spider exoskeleton is sulfurized, labile tissues are decayed, other volatile compounds are driven off, and the spider is flattened due to sediment compaction after

being buried at the lake bottom (Olcott *et al.*, 2022). This taphonomic pathway may have been present in many lakes during the Cenozoic, evidenced by how many compression-type fossils have been observed from other diatom-rich deposits (Olcott *et al.*, 2022: fig. 9). However, lake systems may possess multiple possible taphonomic pathways, and thus induce many types of preservation. The variability in the mode of preservation is most likely the result of different taphonomic influences and early diagenetic factors. The pathway leading to compression fossils in the Aix-en-Provence Formation has already been hypothesized to consist of diatom-driven sulfurization, so we here conduct microscopic and chemical analyses of fossil spiders preserved as molds in order to characterize a potentially separate taphonomic pathway responsible for this distinct preservation. We report new evidence of microbial mats suggesting prolific microbial activity during the deposition of the Aix-en-Provence Formation and we hypothesize that microbial mats played an important role in moldic preservation of these fossil spiders. Compared with the diatomaceous preservation of the compression-type fossil spiders, we suggest that the mat-facilitated moldic preservation reflects deposition in a distinct paleoenvironment.

Geological setting

This study uses fossil spiders preserved in paper-thin sheet-like laminations (0.1–0.5 mm thick) from the Oligocene Aix-en-Provence, France, Lagerstätte (43°31'48"N, 5°23'24"E). The 22.5 Ma Aix-en-Provence Formation is represented by a 150-m succession of informally named subunits (Nury, 1987; Gaudant *et al.*, 2018). The abundant fossil insects come from the aptly-named Insect Bed, which, in turn, is part of the Calcaires & Marnes à Gypse d'Aix; *i.e.*, limestones and gypsum marls. Underlying the Insect Bed are several distinct layers of gypsum and marlstone (Murchison & Lyell, 1829). The Insect Bed is roughly 80-cm thick and represented by thinly laminated light grey and light green calcareous marlstone. There are no reported trace fossils or evidence of bioturbation, and, as a result, the extremely thin laminations are well-preserved and continuous. Overlying the Insect Bed is another fossiliferous layer of light brown marlstones known as La Feuille à Poissons, *i.e.*, the fish layer, that is rich in fossil fishes (Saporta, 1889).

Material and methods

Specimens studied here were loaned to one of us (PAS) and are deposited in the National Museum of Natural History, Paris, France. The specimens are extremely delicate and had been glued to pieces of notecard before the start of

this study in order to protect them from breaking. List of specimens: Aix-1, Aix-32 (with thin section), Aix-10 (part and counterpart), and Aix-24.

Fossils were photographed with a Canon EOS 5D Mark II digital camera attached to a copy stand and the same camera attached to a Leica M650C microscope and viewed in low angle light to enhance details not easily seen. A pieces of matrix material from Aix-32 was embedded in epoxy to make a thin section. The thin section does not cut through the fossil. The thin section was prepared in the Rock Crushing Laboratory at the University of Kansas (KU). Fluorescence imaging was done with an Olympus BX51 Petrographic Scope with a mercury vapor-arc-discharge lamp, and two exciter filters designed to transmit in the UV (330–385 nm wavelength) and violet-blue (400–440 nm wavelength) region. Stacked and stitched images were created using Stream Essentials software. Scanning electron microscopy (SEM) and energy-dispersive x-ray spectroscopy (EDS) analyses of Aix-24 and Aix-32 were conducted at the KU Microscopy and Analytical Imaging Laboratory. Each fossil specimen and the thin section slide were sputter-coated with iridium and mounted on individual aluminum stubs with copper tape for image acquisition. Images and analyses were acquired on a Cold Field Emission Scanning Electron Microscope, Hitachi High Technologies, SU8230 series, with a YAB backscattered electron (BSE) detector, at accelerating voltages ranging from 1.0 to 2.0 kV. EDS used a Silicon Drift Detector (SDD) to create elemental maps. High resolution image mapping of Aix-10 was conducted at University of Missouri X-ray Microanalysis Laboratory; sample Aix-10 was analyzed uncoated, mounted directly to an aluminum stage plate using copper tape, and analyzed using a field emission Zeiss Sigma 500VP. Beam and chamber conditions were as follows: low-vacuum chamber pressure = 25 Pa with a dry nitrogen (99.999%) atmosphere; sample working distance 9.5 ± 0.7 mm; beam accelerating voltage = 20 keV, beam current = 40 nA; 60 μ m aperture. Imaging was conducted with a high-definition 5-segment backscatter detector and a cascade current low-vacuum secondary electron detector, including large-area image mosaics compiled using the ATLAS workflow (Fibics Inc.). EDS elemental mapping was conducted with dual, co-planar Bruker XFlash 6|30 SDD spectrometers used in tandem for 600 s live time.

Results

Bedding surfaces

The bedding surfaces of the samples exhibit a variety of textures in the matrix surrounding the fossils, while the fossils themselves exhibit varying relief depending on the mode of preservation (Fig. 1). The matrix includes wrinkled and pustular textures as well as small fragments

and chips (Fig. 1A, B). The fossils are preserved as internal and external molds. External molds are concave impressions in the matrix that show the appearance of the external features like setae. The distal podomeres of the legs of the spider in Aix-32 are preserved as external molds, while proximal portions of the legs are preserved as internal molds (Fig. 1C). The ventral side of the

cephalothorax is visible and includes internal molds of the sternum, chelicerae, and coxae. The legs of Aix-10 also contain external and internal molds. Some internal molds are preserved in high relief (Fig. 1D, E). The areas of highest relief in the fossils are in the cephalothorax of the spiders, but external features of the cephalothorax, such as eyes, are absent. The cephalothorax is a high relief

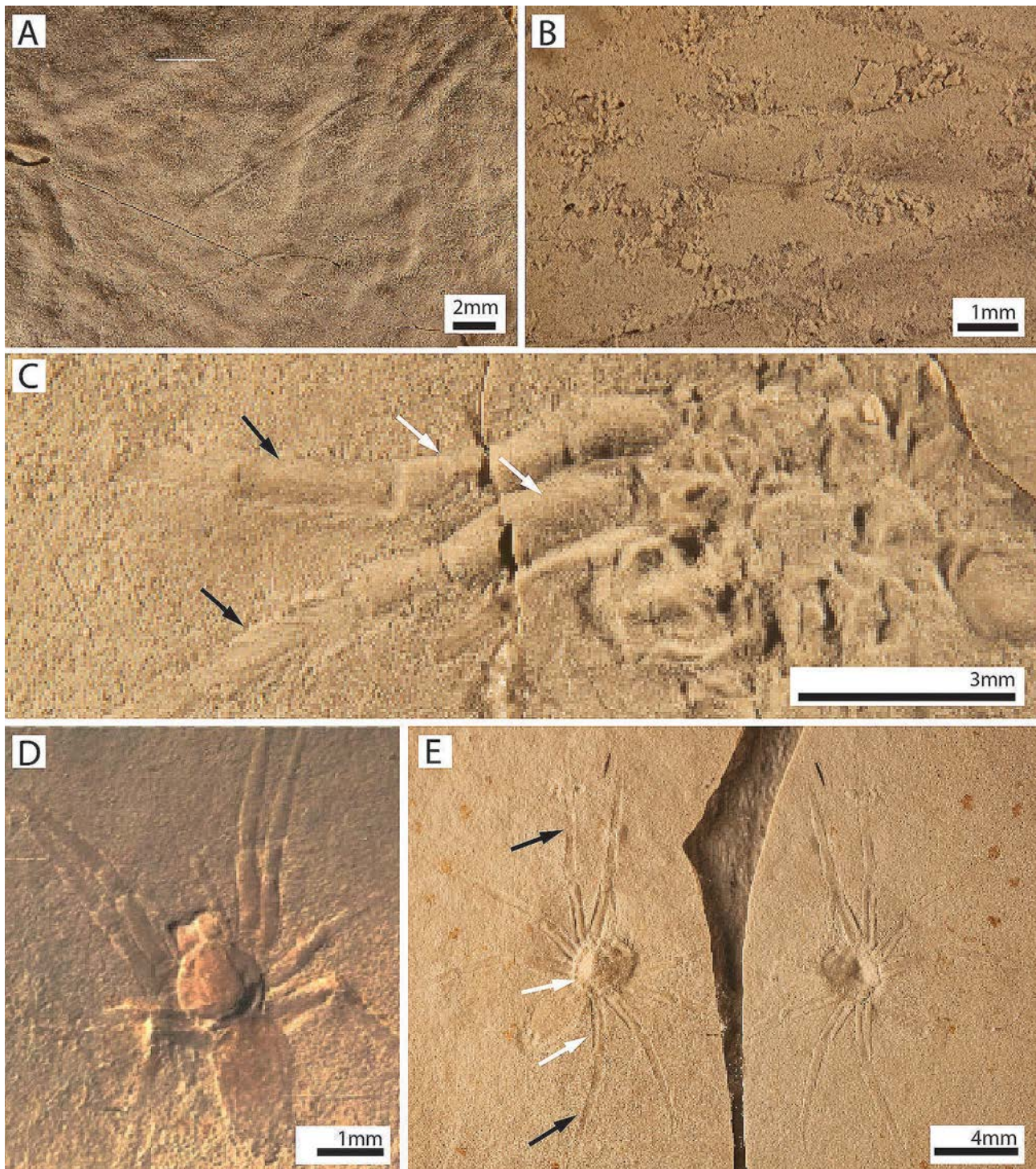


FIGURE 1. Fossil spiders from the Aix-en-Provence Fossil-Lagerstätte. **A**, Aix-1, Wrinkled and pustular (bumps) texture on the bedding surface in the matrix around the fossil. **B**, Aix-32, Small possible microbial mat chips around the legs of a fossil spider. **C**, Aix-32, Spider preserved ventral side visible with external molds (black arrow) and internal molds (white arrow) on legs. **D**, Aix-24, Fossil spider in dorsal side visible view. **E**, Aix-10, Part and counterpart of fossil spider with external molds (black arrows) and internal molds (white arrows).

internal mold with chelicerae visible, and the abdomen is flattened. The spider in Aix-24 is mostly preserved as an internal mold. The cephalothorax is in high relief, with an even higher raised area along the midline, and the chelicerae are projected slightly forward. The abdomen is also flat.

Petrography and fluorescence microscopy

In the thin section of Aix-32, the internal architecture appears as wrinkled laminations. A vertical crack is present in the sample and narrows as it terminates with laminations bending downward along the crack (Fig. 2 B). The sample vibrantly autofluoresces bright blue in UV light and bright green under illumination by blue-violet light (Fig. 2B, C). More detail is revealed with fluorescence microscopy, as compared to plain light, and the sample appears as overlapping tubular slivers (100–200 µm) interspersed with rounded globular masses (15–20 µm) (Fig. 2C, D).

Scanning Electron Microscopy

A backscattered electron (BSE) image of the Aix 32 thin-section reveals the laminae are composed of structures with a variety of shapes (Fig. 3). The most abundant are circular hollow structures (100–200 µm) and elongated structures that are tubular and filamentous and range in size from 200–600 µm. The composition of these structures is C and O, and lacks Ca and Si, and they appear embedded within a C-rich matrix. These circular and elongated structures also have numerous small (20 µm long, 1–3 µm wide) filaments connecting them to each other and to the matrix (Fig. 3D, E). The top layer of the sample lacks these structures and contains abundant small (approx. 40 µm) grains that appear bright white in BSE and are composed of Si and O. Elongated grains (200–300 µm), distinct from the elongated tubular and filamentous structures, that appear bright in BSE are scattered throughout the matrix, but not present in the topmost layer. These grains are composed of Si, O, Mg, Al, and Fe. The C and O-rich tubular and globular structures define distinct laminae within the sample, and Cl, though less abundant, appears to be more concentrated in some layers. The Ca signal is extremely weak and does not appear concentrated in any specific areas.

Sample Aix-10 is composed of tiny mineral grains (2–15 µm) and contains an abundance of circular concave molds (40–50 µm) that are present both on the fossil and in the surrounding matrix (Fig. 4). A net-like pattern is present on the abdomen of the spider. Setae are visible at the posterior of the abdomen and on the legs. The body of the fossil is composed mostly of Ca, C, and O, with S and P concentrated in the abdomen of the spider. The surrounding matrix includes these elements as well as Si, Fe, Al, and K.

The composition of Aix-24 is similar to Aix-10 (Fig. 5). The most abundant elements present are O (51.8

wt%), Ca (25.9 wt%), and C (17.4 wt%) and Si (2.7 wt%). The fossil is composed of O, Ca, and C, while Si is mostly absent in the body of the fossil, and instead is abundant in the matrix. Other elements like Al, Mg, Fe, and K are less abundant (< 1 wt%), but dispersed evenly through the sample. Phosphorus (0.2 wt%) was present in the cephalothorax, but not in the legs. Two kinds of microtextures are observed in the body of the fossil: crystals (100 µm) with a platy habit, and small (20 µm) spheroids (Fig. 5C, D). The small spheroids are composed of Ca (43.6 wt%), O (40.8 wt%), C (7.4 wt%), and Si (6.5 wt%). Centric diatom valves and fragments of girdles are also present in the sample, which are composed of silica (Fig. 5E, F). These diatoms possess relatively few punctae in the center and smaller more abundant punctae near the distal margins of the valves.

Discussion

Evidence of microbial mats

The textures of the bedding surfaces, tubular and globular structures observed in thin section, spheroids, diatoms, and chemistry suggests microbial mats and microbiotic activity were prevalent during the deposition in the Oligocene Aix-en-Provence basin of France. The wrinkled and pustular textures observed on the bedding surfaces of Aix-1 are documented in other fossil and modern microbial mats (Schieber, 1998; Retallack *et al.*, 2012). The wrinkled texture resembles Kinneyia-type wrinkles observed in the rock record (Porada *et al.*, 2008). The pustular texture appears as small irregular bumps in modern and fossil microbial mats and may represent poorly lithified sheets deposited nearshore (Retallack *et al.*, 2012; Suosaari *et al.*, 2016). The small fragments are likely microbial mat chips, where pieces of the microbial mat tear and are ripped up and redeposited (Noffke *et al.*, 2013). The mat chips in the Aix Formation are irregularly shaped like in other deposits, but are smaller. Microbial mat chips can form in subaerial and subaqueous environments, but commonly are associated with desiccation (Gerdes, 2007).

The matrix fabric of specimen Aix-32 resembles a thrombolitic texture in UV light, but the fluorescence response is so strong that it overshadows the distinct tubes and structures visible in BSE imaging. Many of the elongated and tubular structures in the matrix closely resemble filamentous microbial sheaths and also contain many small filaments connecting them to each other and the surrounding matrix similar to the structure of some EPS (Chafetz & Buczynski, 1992; DeFarge *et al.*, 1996; Chan *et al.*, 2016; Mei *et al.*, 2020). The equally high C and O, but low Ca, composition of this material excludes

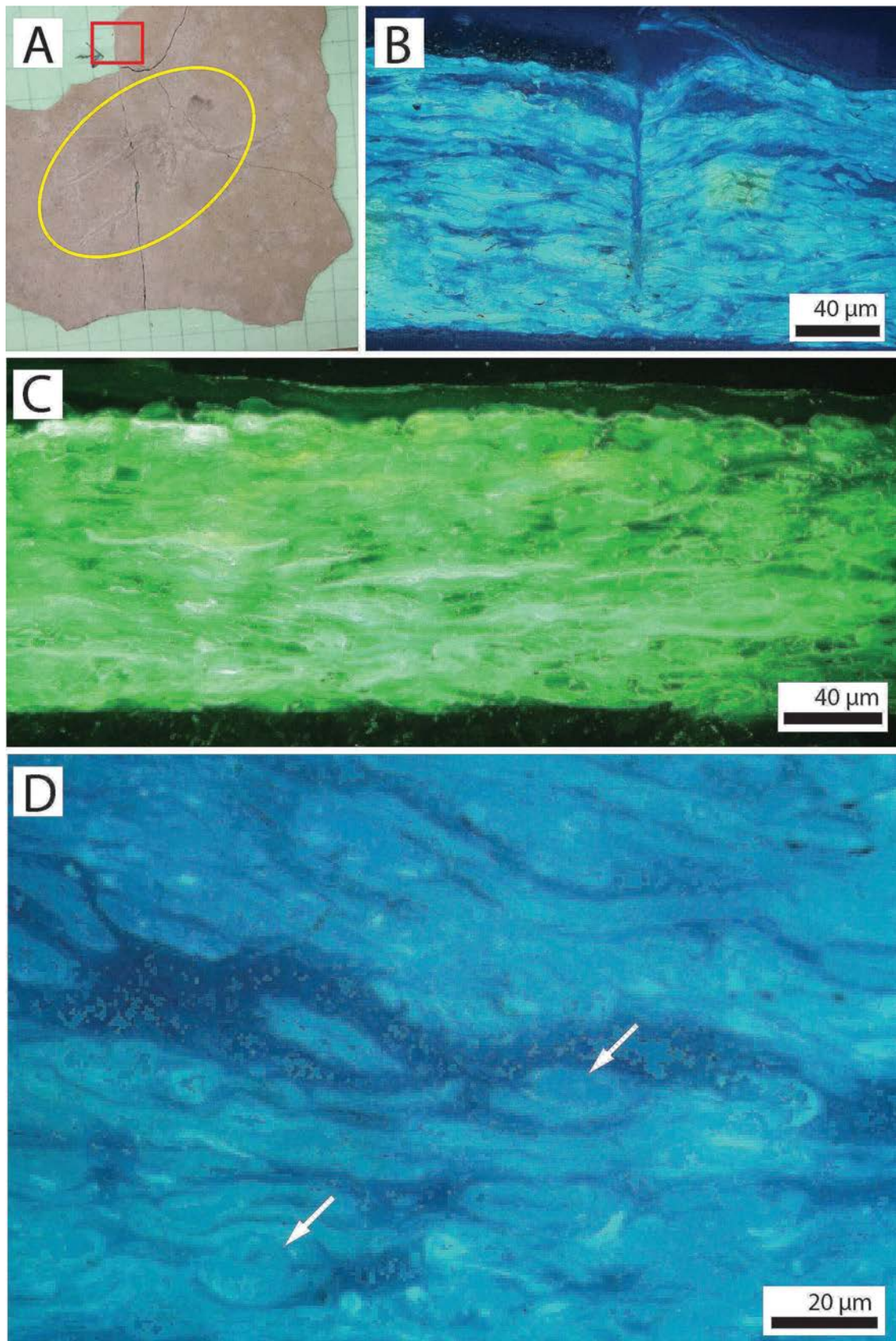


FIGURE 2. Specimen Aix-32 and various areas of its thin section viewed with fluorescence microscopy. **A**, Fossil sample with red box indicating area where thin section was cut. Because the fossil is hard to see, a yellow oval is around the fossil spider. **B**, Bright blue autofluorescence of thin section in ultraviolet (UV) light showing laminae and vertical crack. **C**, Bright green autofluorescence in violet-blue light. **D**, Magnified image of Aix-32 thin section in UV light showing long narrow slivers and circular masses (white arrows).

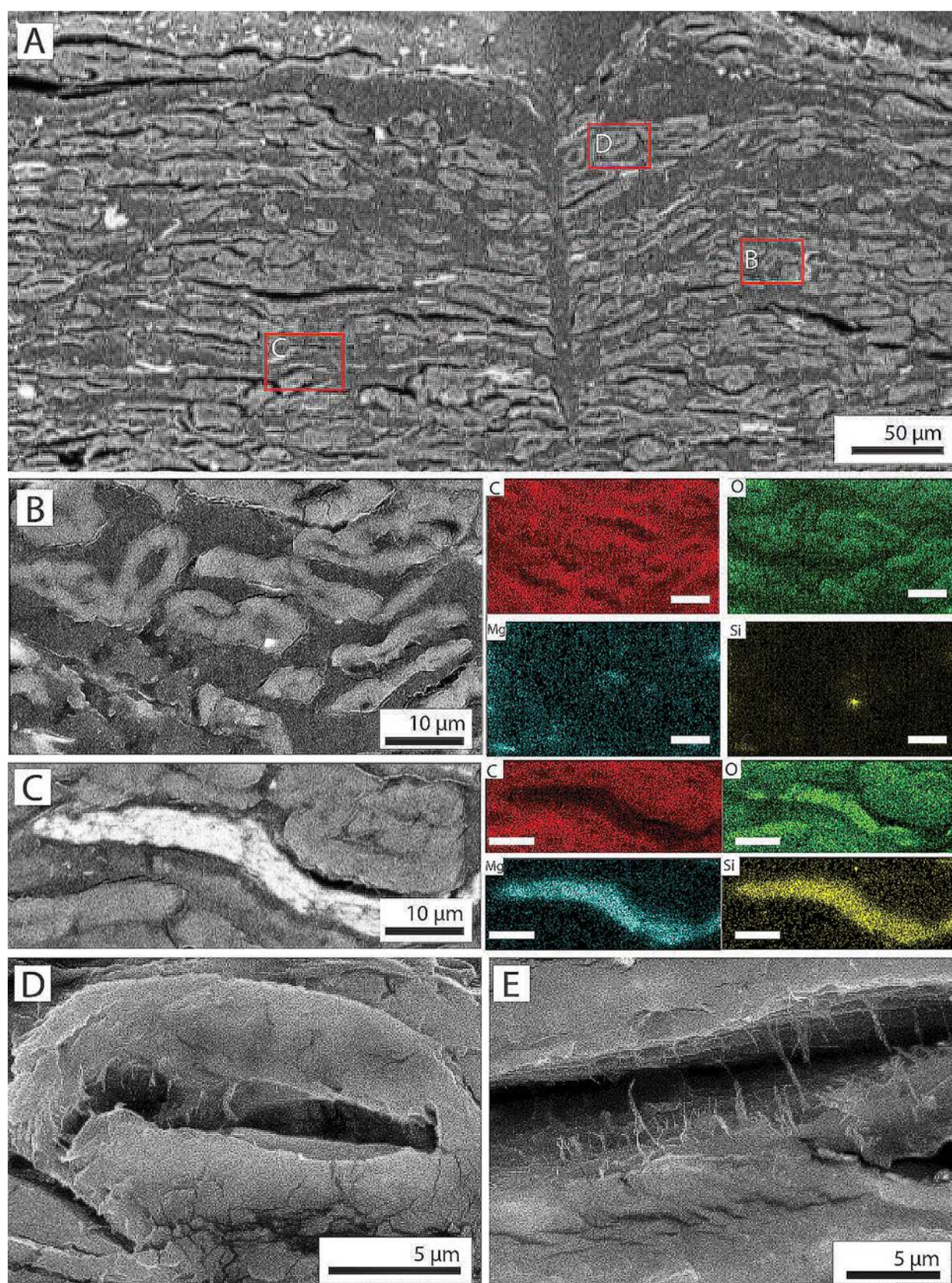


FIGURE 3. Scanning electron microscopy and chemical analyses of Aix-32 thin section. **A**, BSE image of vertical crack and small white granules (top) in uppermost layer. Red boxes indicate location of corresponding images and letters. **B**, BSE image and elemental maps of tubular structures that are composed mostly of C and O (white bars are 10 µm). **C**, BSE image and elemental maps of tubular structures with one tube composed of Mg, Al, Fe, Si, and Fe in contrast to the C and O-rich surrounding tubes (white bars are 10 µm). **D**, Magnified BSE image of one of the circular structures. **E**, BSE image of filamentous structures between tubes (location in image **A** unknown).

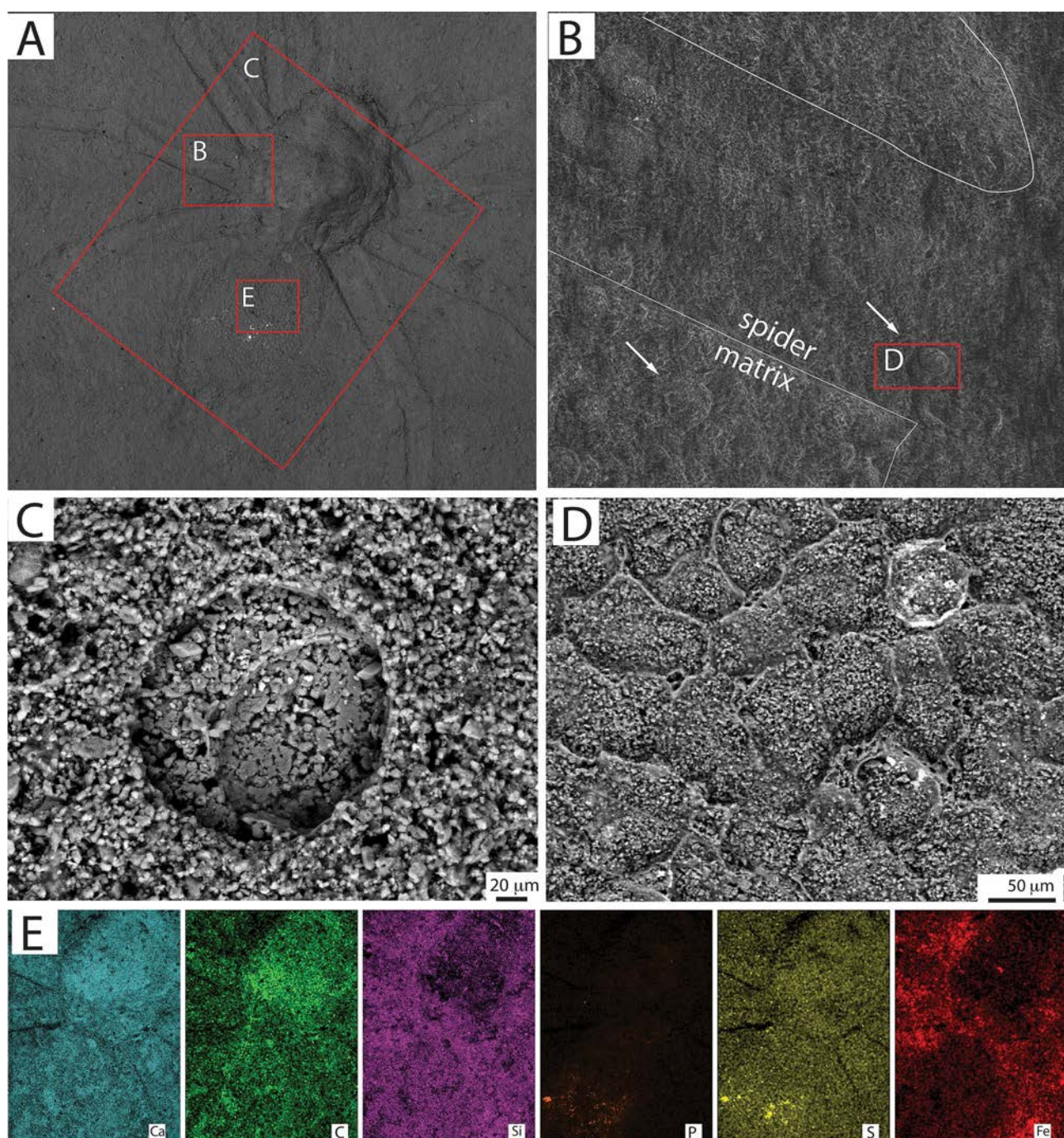


FIGURE 4. BSE images and elemental maps of Aix-10. **A**, BSE image of fossil spider with red boxes indicating locations of corresponding images and letters. **B**, BSE image of fossil spider legs and surrounding matrix with circular concave impressions in matrix and on spider body. **C**, Close up of circular impression and the small granules that comprise the specimen. **D**, Close up of net-like pattern on the abdomen of the spider. **E**, Elemental maps of the fossil and matrix. Most elements are present throughout the sample except for P which is limited to the fossil spider body. Si and Fe are mostly present in the matrix around the fossil.

calcium carbonate as an abundant mineral in Aix-32. This matrix fabric differs from what extremely thin and flat laminae reported in compression fossils from the Aix-en-Provence Formation (Olcott *et al.*, 2022, fig. 4).

The bright white structures in BSE images of Aix-32 are likely clays, and more specifically, illite ((K,H₃O)(Al,Mg,Fe)₂(Si,Al)₄O₁₀[(OH)₂(H₂O)]). The clay masses are scattered throughout the sample, but one of the tubular

structures appears to be replaced entirely by illite (Fig. 3). Illite has been found in other fossiliferous deposits and is commonly connected to microbial precipitation and influence (Gabbott *et al.*, 2001; Briggs, 2003).

The rhombohedral/platy crystals suggest bacterially-induced precipitation of calcite, while spherules suggest direct carbonate precipitation by microbes (Dupraz *et al.*, 2009). Rhomboids and spherules have been produced by

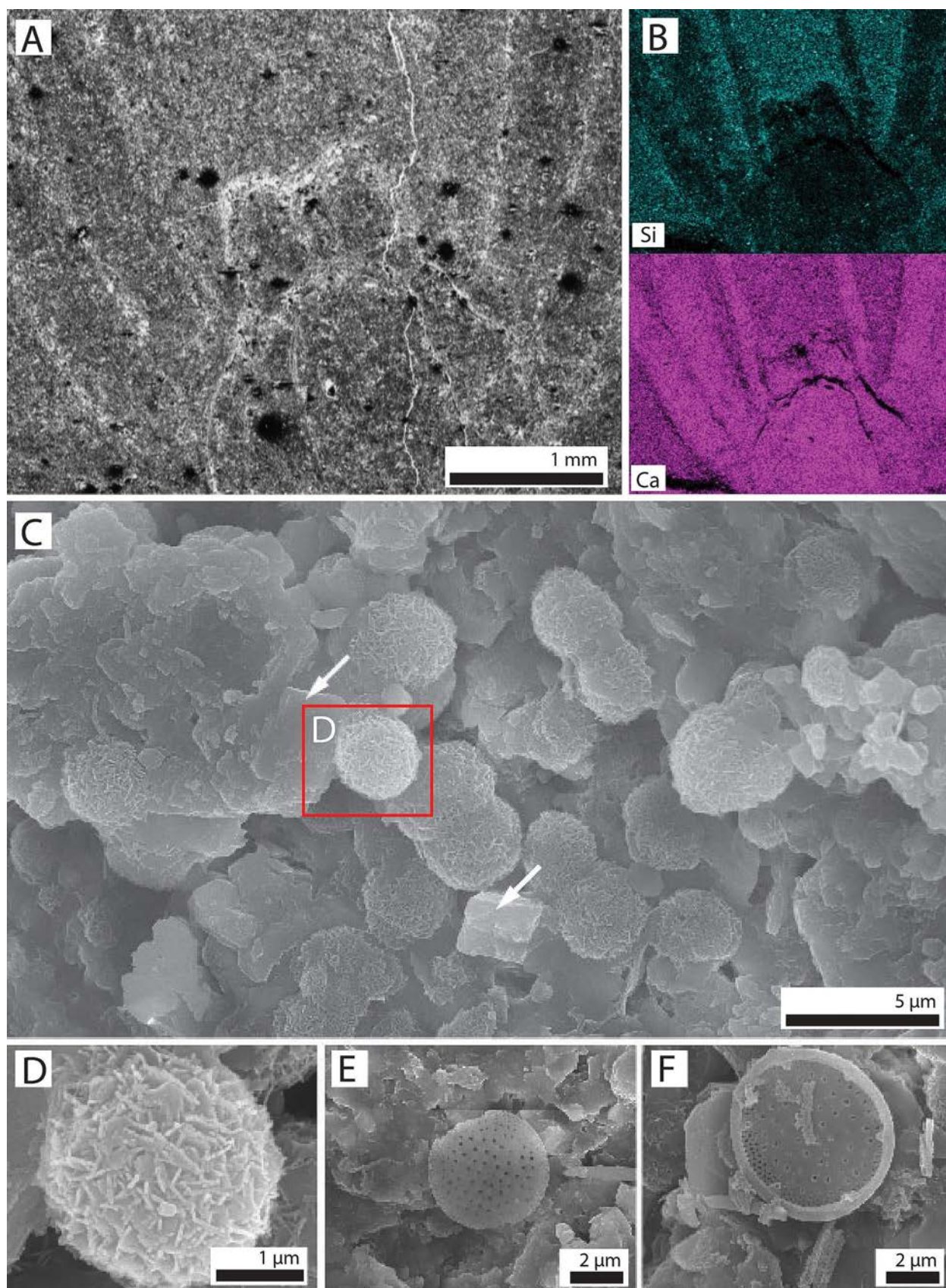


FIGURE 5. BSE images and elemental maps of Aix-24. **A**, BSE image anterior part of spider. **B**, Si and Ca elemental maps of Aix-24 showing Ca present everywhere and Si mostly present in matrix around spider body. **C**, BSE image of rhomboid crystals (white arrow) and many spheroids on the body of the fossil spider. Red box indicates location of image **D**. **D**, Magnified BSE image of spheroid showing a surface that appears to be covered in structures with a morphology that resembles bacteria. **E**, BSE image of single diatom valve. **F**, BSE image of a diatom valve and girdle fragments.

microbes experimentally, but spherules have also been interpreted as coccoidal bacterial cells (Wei *et al.*, 2015; Warren *et al.*, 2016; Meier *et al.*, 2017). The spherules observed here resemble spherules found in carbonate microbialites and filamentous bacteria (Perri & Tucker, 2007; Perri & Spadafora, 2011). Both carbonate rhombs and spherules are interpreted as the result of passive microbially influenced precipitation, yet here, filamentous bacteria are an extremely abundant component of the spherules and appear to be autolithified.

Based on the size, morphology, and presence of fragmented diatoms, the numerous circular voids in Aix-10 likely represent centric diatoms that have been removed through dissolution. The reason for their dissolution in the mold fossils may be a much later diagenetic consequence after burial, but diatom frustules have also been shown to dissolve in microbial mats due to localized elevated pH (Palm, 2018). While these diatoms are abundant in the mold fossils examined here, their arrangement differs from the pennate diatoms previously reported in compression fossils from the Aix-en-Provence Formation (Olcott *et al.*, 2022). In contrast to the dense mats of diatoms in the compression fossils, these diatoms do not appear to form mats and, instead, are likely just background fallout of diatoms in the water column as evidenced by their presence in both the fossils and the matrix. Diatoms have also been reported from the Shanwang Lagerstätte, China, where insect exoskeletons are preserved with a high level of detail in diatomite (Hu *et al.*, 2019). The diatoms in Shanwang fossils, however, are still intact and have not dissolved. Diatoms have been hypothesized to help trap and sink insects and spiders due to their sticky and mucilaginous nature and even create anoxic microenvironments that reduce decay, but there is no evidence to suggest the centric diatoms in these samples contribute to the formation of the 3D mold fossils in this deposit (Harding & Chant, 2000; O'Brien *et al.*, 2008).

Fossil preservation quality

3D moldic preservation of fossil spiders in lacustrine deposits is rare compared to compression fossils, but is observed in the Bembridge Marls from the Isle of Wight (Eocene). Isle of Wight arthropods are preserved as mineralized 3D calcified replacements with aliphatic organic material (McCobb *et al.*, 1998). Cuticle-lined voids were also reported, and may represent the early formation of concretions to keep carcasses from collapsing, and thus preserving their 3D structure. Muscle fibers and cuticle texture are preserved in the Isle of Wight fossils, much greater detail than in Aix-en-Provence, suggesting the rapid mineralization of internal and external remains (Selden, 2001). The Aix-en-Provence spiders preserved as molds lack this level of detail and therefore, were likely not rapidly mineralized. The microbial mats may have

produced mineralized crusts of calcite around the spiders based on the composition of the samples.

High relief internal molds of fossil spiders have not been reported from other spider-bearing Lagerstätten. Fossil insects and spiders from the Lower Cretaceous Crato Formation of Brazil are preserved as 3D goethite replacements with internal voids filled with calcite and can be relatively high relief (Selden *et al.*, 2006; Downen & Selden, 2021). The preservation of arthropods in the Crato Formation was likely facilitated by microbial mats (Varejão *et al.*, 2019; Barling *et al.*, 2020; Iniesto *et al.*, 2021; Dias & Carvalho, 2022). However, the internal anatomy of the cephalothorax of the Crato spiders are preserved in contrast to the Aix-en-Provence spider molds. The lack of visible structure in the cephalothorax of Aix-en-Provence spiders suggests the internal anatomy was not preserved. Instead, the fossils resemble a steinkern-like (German: *Stein* (“stone”) + *Kern* (“kernel, nucleus”)) mode of preservation.

Taphonomic pathway and paleoenvironment

Microbial mats are complex associations of biofilms, composed of communities of various species of microbes, and often associated with a matrix of extracellular polymeric substances (EPS), that are hypothesized to play a significant role in soft-bodied preservation (Stolz, 2000; Briggs, 2003; Janssen *et al.*, 2022). Microbial mats may aid in the process of fossilization in several ways: stabilizing sediment and carcasses, directly precipitating minerals on the surface of remains or replacing organic remains, inducing precipitation of minerals by altering the surrounding chemistry of the environment, and/or reducing scavenging and decay (Gall, 1990; Wilby *et al.*, 1996; Martinez-Delclòs *et al.*, 2004). Actualistic experiments have demonstrated that microbial mats help preserve soft tissues and can fossilize material rapidly, supporting their involvement of exceptional preservation in ancient environments (Briggs & Kear, 1993; Sagemann *et al.*, 1999; Darroch *et al.*, 2012; Iniesto *et al.*, 2016, 2021). Microbial mats are hypothesized to play a role in fossilization in several spider-bearing Lagerstätten including the Crato Formation of Brazil, Florissant Formation of Colorado, and the Kishenehn Formation of Montana (O'Brien *et al.*, 2002, 2008; Greenwalt *et al.*, 2014; Dias & Carvalho, 2022).

The interpreted paleoenvironment of the Aix-en-Provence Formation is a brackish lacustrine/lagoonal setting with varying salinity and hosting a diverse paleoecosystem (Gaudant *et al.*, 2018). Various types of fish suggest brackish conditions in a lagoonal setting, but episodes of freshwater lacustrine settings are supported by the presence of frogs and turtles in the Insect Bed (Piveteau, 1927; Gaudant, 1978; Fontes *et al.*, 1980). Fluctuating salinity is also supported by mass mortality

events. Fossil fish and dragonfly nymphs occur in great numbers and likely represent mass die-off events plausibly from rapid changes in salinity (Nury, 1987; Gaudant *et al.*, 2018). The plant and insect assemblages are indicative of a warm subtropical paleoclimate (Gregor & Knobloch, 2001; Collomb *et al.*, 2008). The flora includes water lilies (Nymphaeaceae), banana trees (Musaceae), pine trees (Pinaceae), and palm leaf trees (Malpighiaceae), many of which resemble modern day species from Africa (de Saporta, 1889). Beetles (Coleoptera), flies (Diptera), and wasps (Hymenoptera) are the most abundant insects, but spiders are also relatively abundant and include wolf spiders (Lycosidae), crab spiders (Thomisidae), and long-jawed orbweavers (Tetragnathidae) (Gourret, 1887).

These water bodies are dynamic systems that are sensitive to changes in climate and environment, and thus can vary in chemistry, salinity, depth, biotic composition, and other parameters (Street-Perrott & Harrison, 1985; Kemp, 1996; Cohen, 2003). Many of the conditions that can promote soft tissue preservation, such as anoxia, rapid burial, rapid mineralization, and microbial mats, are likely to be present in lakes (Martínez-Delclòs *et al.*, 2004; Smith, 2012). With so many different conditions and parameters, the taphonomic pathways responsible for fossil preservation in lakes can be highly varied and may result in variable modes of preservation (*e.g.*, molds, replacements, compressions) that may fluctuate both between and within deposits.

In a taphonomic pathway leading to molds, the spiders that enter the Aix-en-Provence paleolake likely sink to the bottom of the lake and are deposited on calcium carbonate-producing microbial mats. The spiders create an impression in the mat on which they land leading to the preservation of external features such as setae; This has been demonstrated experimentally with setae from insects (Iniesto *et al.*, 2016). Next, microbes colonize and envelope the spider carcasses. The more robust sclerotized parts of the spider (legs and carapace) retain their 3D form longer, while the abdomen, which is softer, is flattened. The internal soft tissues of the spiders decay so that no internal organs or structures are preserved, and the void space is filled in with microbial mat material and carbonate (Martínez-Delclòs *et al.*, 2004). Any remaining cuticle or other parts of the exoskeleton is removed later through diagenesis and the microbial mats are eventually lithified. When the laminations are split, the fossils preferentially break along the boundary between the mold and the overlying microbial mat, typically in high relief.

The results from this study provide additional interpretations to the paleoenvironment of the Aix-en-Provence Formation. Pustular microbial mat textures are found in peritidal settings (Gerdes *et al.*, 2001). Microbial mat chips suggest a shallow paleolake with periods of very shallow water and possibly subaerial conditions

(Gerdes *et al.*, 2000). Particularly shallow conditions may correspond to episodes of increasing salinity. These increases in salinity may also be tied to mass mortality events of fishes and dragonfly nymphs (Gaudant *et al.*, 2018). This evidence supports a shallow lacustrine or lagoonal setting, with possible episodes of subaerial exposure and fluctuating salinity.

Unfortunately, the fossils from Aix-en-Provence were collected without stratigraphic context. As a result, it is unknown if the differing lithologies and their corresponding modes of preservation are related to changes in the paleoenvironment through time or reflect different localized environments within the paleolake such as nearshore or offshore. For taphonomic studies and their paleoenvironmental implications, it is critical to collect detailed stratigraphic data. While it is unknown if the spiders in this study are from the exact same time, these results described here suggest that multiple complex taphonomic pathways existed during the depositional history of the Aix-en-Provence Formation.

Conclusion

The Oligocene Aix-en-Provence Formation of France is a Lagerstätten with an abundance of exceptionally preserved soft-bodied organisms including spiders preserved as compressions and molds. A diatom-sulfurization model for the preservation of spiders as compression fossils was recently described, and now new evidence supports a hypothesis that microbial mats promote preservation as internal and external molds. Evidence of microbial mats include pustular textures and microbial mat chips on the bedding surfaces and microbial sheaths and bacterial spheroids in the matrix. Centric diatoms are present alongside mold fossils, but unlike the mat-forming diatoms hypothesized to play an important role in preservation as compressions, the diatoms here are unlikely to be a control on preservation. The spider fossils investigated previously and here suggest that the paleoenvironment of the Aix-en-Provence Formation was dynamic and at least two possible taphonomic pathways were present and responsible for differing modes of preservation.

Acknowledgements

The authors thank Dr. André Nel (National Museum of Natural History, France) for loaning the specimens; Pike Hollman (University of Kansas) for making thin sections; Dr. Prem Thapa-Chetri and the KU Microscopy and Analytical Imaging Laboratory for electron microscopy sample prep and imaging; Evolving Earth Foundation

for funding. This paper is dedicated to Professor David Grimaldi, in honor of his impressive contribution to fossil insects and Diptera evolution

References

- Allison, P.A. (1988) Konservat-Lagerstätten: cause and classification. *Paleobiology*, 14, 331–344.
<https://doi.org/10.1017/S0094837300012082>
- Allison, P.A. & Briggs, D.E.G. (1993) Exceptional fossil record: Distribution of soft-tissue preservation through the Phanerozoic. *Geology*, 21, 527–530.
[https://doi.org/10.1130/0091-7613\(1993\)021<0527:EFRDOS>2.3.CO;2](https://doi.org/10.1130/0091-7613(1993)021<0527:EFRDOS>2.3.CO;2)
- Barling, N., Martill, D.M. & Heads, S.W. (2020) A geochemical model for the preservation of insects in the Crato Formation (Lower Cretaceous) of Brazil. *Cretaceous Research*, 116, 104608.
<https://doi.org/10.1016/j.cretres.2020.104608>
- Briggs, D.E.G. (2003) The role of decay and mineralization in the preservation of soft-bodied fossils. *Annual review of earth and planetary sciences*, 31, 275–301.
<https://doi.org/10.1146/annurev.earth.31.100901.144746>
- Briggs, D.E. & Kear, A.J. (1993) Fossilization of soft tissue in the laboratory. *Science*, 259, 1439–1442.
<https://doi.org/10.1126/science.259.5100.1439>
- Chafetz, H.S. & Buczynski, C. (1992) Bacterially induced lithification of microbial mats. *Palaos*, 7, 277–293.
<https://doi.org/10.2307/3514973>
- Chan, C.S., McAllister, S.M., Leavitt, A.H., Glazer, B.T., Krepski, S.T. & Emerson, D. (2016) The architecture of iron microbial mats reflects the adaptation of chemolithotrophic iron oxidation in freshwater and marine environments. *Frontiers in Microbiology*, 7, 796.
<https://doi.org/10.3389/fmicb.2016.00796>
- Cohen, A.S. (2003) *Paleolimnology: The history and evolution of lake systems*. Oxford University Press, 528 pp.
<https://doi.org/10.1093/oso/9780195133530.001.0001>
- Collomb, F.-M., Nel, A., Fleck, G. & Waller, A. (2008) March flies and European Cenozoic palaeoclimates (Diptera: Bibionidae). *Annales de la Société entomologique de France, Société entomologique de France*, 44, 161–179.
<https://doi.org/10.1080/00379271.2008.10697553>
- Darroch, S.A.F., Laflamme, M., Schiffbauer, J.D. & Briggs, D.E.G. (2012) Experimental formation of a microbial death mask. *Palaos*, 27, 293–303.
<https://doi.org/10.2110/palo.2011.p11-059r>
- DeFarge, C., Trichet, J., Jaunet, A.-M., Robert, M., Tribble, J. & Sansone, F.J. (1996) Texture of microbial sediments revealed by cryo-scanning electron microscopy. *Journal of Sedimentary Research*, 66, 935–947.
<https://doi.org/10.1306/D4268446-2B26-11D7-8648000102C1865D>
- Dias, J.J. & Carvalho, I. de S. (2022) The role of microbial mats in the exquisite preservation of Aptian insect fossils from the Crato Lagerstätte, Brazil. *Cretaceous Research*, 130, 105068.
<https://doi.org/10.1016/j.cretres.2021.105068>
- Downen, M.R. & Selden, P.A. (2021) The earliest palpimanid spider (Araneae: Palpimanidae), from the Crato Fossil-Lagerstätte (Cretaceous, Brazil). *Arachnologische Mitteilungen*, 49, 91–97.
<https://doi.org/10.1636/JoA-S-19-059>
- Dupraz, C., Reid, R.P., Braissant, O., Decho, A.W., Norman, R.S. & Visscher, P.T. (2009) Processes of carbonate precipitation in modern microbial mats. *Earth-Science Reviews*, 96, 141–162.
<https://doi.org/10.1016/j.earscirev.2008.10.005>
- Fontes, J.-C., Gaudant, J. & Truc, G. (1980) Données paléocéologiques, teneurs en isotopes lourds et paléohydrologie du bassin gypsifère oligocène d'Aix-en-Provence. *Bulletin de la Société géologique de France*, 7, 491–500.
<https://doi.org/10.2113/gssgfbull.S7-XXII.3.491>
- Gabbott, S.E., Norry, M.J., Aldridge, R.J. & Theron, J.N. (2001) Preservation of fossils in clay minerals; a unique example from the Upper Ordovician Soom Shale, South Africa. *Proceedings of the Yorkshire Geological Society*, 53, 237–244.
<https://doi.org/10.1144/pygs.53.3.237>
- Gall, J.-C. (1990) Les voiles microbiens. Leur contribution à la fossilisation des organismes au corps mou. *Lethaia*, 23, 21–28.
<https://doi.org/10.1111/j.1502-3931.1990.tb01778.x>
- Gaudant, J. (1978) Sur les conditions de gisement de l'ichthyofaune oligocène d'Aix-en-Provence (Bouches-du-Rhône): Essai de définition d'un modèle paléocéologique et paléogéographique. *Geobios (Memoire special)*, 11, 393–397.
[https://doi.org/10.1016/S0016-6995\(78\)80039-4](https://doi.org/10.1016/S0016-6995(78)80039-4)
- Gaudant, J., Nel, A., Nury, D., Véran, M. & Carnevale, G. (2018) The uppermost Oligocene of Aix-en-Provence (Bouches-du-Rhône, Southern France): A Cenozoic brackish subtropical Konservat-Lagerstätte, with fishes, insects and plants. *Comptes rendus Palevol*, 17, 460–478.
<https://doi.org/10.1016/j.crpv.2017.08.002>
- Gerdes, G. (2007) Structures left by modern microbial mats in their host sediments. In: *Atlas of microbial mat features preserved within the siliciclastic rock record*. Elsevier, Amsterdam, pp. 5–38.
- Gerdes, G., Klenke, T. & Noffke, N. (2001) Microbial signatures in peritidal siliciclastic sediments: a catalogue. *Sedimentology*, 47, 279–308.
<https://doi.org/10.1046/j.1365-3091.2000.00284.x>
- Gerdes, G., Krumbein, W.E. & Noffke, N. (2000) Evaporite Microbial Sediments. In: Riding, R.E. & Awramik, S.M. (Eds), *Microbial Sediments*. Springer, Berlin, Heidelberg, pp. 196–208.
https://doi.org/10.1007/978-3-662-04036-2_22
- Gourret, P. (1887) Recherches sur les arachnides tertiaires d'Aix en Provence. *Recueil Zoologique Suisse*, 4, 431–496.

- Greenwalt, D.E., Rose, T.R., Siljestrom, S.M., Goreva, Y.S., Constenius, K.N. & Wingerath, J.G. (2014) Taphonomy of the fossil insects of the middle Eocene Kishenehn Formation. *Acta palaeontologica Polonica*, 60, 931–948. <https://doi.org/10.4202/app.00071.2014>
- Gregor, H.-J. von & Knobloch, E. (2001) Kritische Bemerkungen zu Saporta's fossilen Floren in Süd-Frankreich, speziell in der Provence. *Flora Tertiaria Mediterranea*, 4, 1–57.
- Gupta, N.S., Michels, R., Briggs, D.E.G., Evershed, R.P. & Pancost, R.D. (2006) The organic preservation of fossil arthropods: an experimental study. *Proceedings of The Royal Society (Biological sciences)*, 273, 2777–2783. <https://doi.org/10.1098/rspb.2006.3646>
- Harding, I.C. & Chant, L.S. (2000) Self-sedimented diatom mats as agents of exceptional fossil preservation in the Oligocene Florissant lake beds, Colorado, United States. *Geology*, 28, 195–198. [https://doi.org/10.1130/0091-7613\(2000\)28<195:SDMAAO>2.0.CO;2](https://doi.org/10.1130/0091-7613(2000)28<195:SDMAAO>2.0.CO;2)
- Hu, L., Xiang, H.Y., Cai, C.Y., Zhao, T., Huang, D.Y. & Pan, Y.H. (2019) High-fidelity preservation of the Scarabaeoidea (Insecta) exoskeletons from the Miocene of Shanwang. *Palaeoentomology*, 2 (1), 94–101. <https://doi.org/10.11646/palaeoentomology.2.1.7>
- Iniesto, M., Buscalioni, Á.D., Carmen Guerrero, M., Benzerara, K., Moreira, D. & López-Archilla, A.I. (2016) Involvement of microbial mats in early fossilization by decay delay and formation of impressions and replicas of vertebrates and invertebrates. *Scientific reports*, 6, 1–12. <https://doi.org/10.1038/srep25716>
- Iniesto, M., Gutiérrez-Silva, P., Dias, J.J., Carvalho, I.S., Buscalioni, A.D. & López-Archilla, A.I. (2021) Soft tissue histology of insect larvae decayed in laboratory experiments using microbial mats: Taphonomic comparison with Cretaceous fossil insects from the exceptionally preserved biota of Araripe, Brazil. *Palaeogeography, Palaeoclimatology, Palaeoecology*, 564, 110156. <https://doi.org/10.1016/j.palaeo.2020.110156>
- Janssen, K., Mähler, B., Rust, J., Bierbaum, G. & McCoy, V.E. (2022) The complex role of microbial metabolic activity in fossilization. *Biological reviews of the Cambridge Philosophical Society*, 97, 449–465. <https://doi.org/10.1111/brv.12806>
- Kemp, A.E.S. (1996) Laminated sediments as palaeo-indicators. *Geological Society, London, Special Publications*, 116, vii–xii. <https://doi.org/10.1144/GSL.SP.1996.116.01.01>
- Martínez-Delclòs, X., Briggs, D.E.G. & Peñalver, E. (2004) Taphonomy of insects in carbonates and amber. *Palaeogeography, Palaeoclimatology, Palaeoecology*, 203, 19–64. [https://doi.org/10.1016/S0031-0182\(03\)00643-6](https://doi.org/10.1016/S0031-0182(03)00643-6)
- McCobb, L.M.E., Duncan, I.J., Jarzembowski, E.A., Stankiewicz, B.A., Wills, M.A. & Briggs, D.E.G. (1998) Taphonomy of the insects from the insect bed (Bembridge Marls), late Eocene, Isle of Wight, England. *Geological magazine*, 135, 553–563. <https://doi.org/10.1017/S0016756898001204>
- Meier, A., Kastner, A., Harries, D., Wierzbicka-Wieczorek, M., Majzlan, J., Büchel, G. & Kothe, E. (2017) Calcium carbonates: induced biomineralization with controlled macromorphology. *Biogeosciences*, 14, 4867–4878. <https://doi.org/10.5194/bg-14-4867-2017>
- Mei, M.X., Latif, K., Mei, C.J., Gao, J.H. & Meng, Q.F. (2020) Thrombotic clots dominated by filamentous cyanobacteria and crusts of radio-fibrous calcite in the Furongian Changshan Formation, North China. *Sedimentary geology*, 395, 105540. <https://doi.org/10.1016/j.sedgeo.2019.105540>
- Murchison, R.I. & Lyell, C. (1829) On the Tertiary fresh-water Formations of Aix, in Provence, including the coal-field of Fuveau, with a description of fossil insects, Shells and Plants, contained therein; by John Curtis, FLS; J. de C. Sowerby, Esq. FLS, and J. Lindley Esq., Professor of Botany in the London University. (Communicated by the Authors). *The Edinburgh New Philosophical Journal*, 7, 287–298.
- Muscente, A.D., Schiffbauer, J.D., Broce, J., Laflamme, M., O'Donnell, K., Boag, T.H., Meyer, M., Hawkins, A.D., Huntley, J.W., McNamara, M., MacKenzie, L.A., Stanley, G.D., Hinman, N.W., Hofmann, M.H. & Xiao, S.H. (2017) Exceptionally preserved fossil assemblages through geologic time and space. *Gondwana Research*, 48, 164–188. <https://doi.org/10.1016/j.gr.2017.04.020>
- Noffke, N., Christian, D., Wacey, D. & Hazen, R.M. (2013) Microbially induced sedimentary structures recording an ancient ecosystem in the ca. 3.48 billion-year-old Dresser Formation, Pilbara, Western Australia. *Astrobiology*, 13, 1103–1124. <https://doi.org/10.1089/ast.2013.1030>
- Nury, D. (1987) *L'Oligocène de Provence méridionale: Stratigraphie, dynamique sédimentaire, reconstitutions paléographiques*. Aix-Marseille 1, 410 pp.
- O'Brien, N.R., Meyer, H.W. & Harding, I.C. (2008) The role of biofilms in fossil preservation, Florissant Formation, Colorado. *Paleontology of the Upper Eocene Florissant Formation, Colorado*, 435, 19–31. [https://doi.org/10.1130/2008.2435\(02\)](https://doi.org/10.1130/2008.2435(02))
- O'Brien, N.R., Meyer, H.W., Reilly, K., Ross, A.M. & Maguire, S. (2002) Microbial taphonomic processes in the fossilization of insects and plants in the late Eocene Florissant Formation, Colorado. *Rocky Mountain Geology*, 37, 1–11. <https://doi.org/10.2113/gsrocky.37.1.1>
- Olcott, A.N., Downen, M.R., Schiffbauer, J.D. & Selden, P.A. (2022) The exceptional preservation of Aix-en-Provence spider fossils could have been facilitated by diatoms. *Communications Earth & Environment*, 3, 1–10. <https://doi.org/10.1038/s43247-022-00424-7>
- Palm, A. (2018) *The dissolution of diatoms in marine microbial mats. Master's Theses*. 1219. Available from: https://opencommons.uconn.edu/gs_theses/1219 (Accessed 15 July 2022)
- Perri, E. & Spadafora, A. (2011) Evidence of microbial

- biomineralization in modern and ancient stromatolites. *In*: Tewari, V. & Seckbach, J. (Eds), *Stromatolites: Interaction of microbes with sediments*. Springer Netherlands, Dordrecht, pp. 631–649.
https://doi.org/10.1007/978-94-007-0397-1_28
- Perri, E. & Tucker, M. (2007) Bacterial fossils and microbial dolomite in Triassic stromatolites. *Geology*, 35, 207–210.
<https://doi.org/10.1130/G23354A.1>
- Piveteau, J. (1927) *Études sur quelques amphibiens et reptiles fossiles*. Masson. Available from: <https://pascal-francis.inist.fr/vibad/index.php?action=getRecordDetail&idt=GEODEB RGMFR2015310> (Accessed 24 May 2022)
- Porada, H., Ghergut, J. & Bouougri, E.H. (2008) Kinneyia-type wrinkle structures—critical review and model of formation. *Palaaios*, 23 (2), 65–77.
<https://doi.org/10.2110/palo.2006.p06-095r>
- Retallack, G.J., Noffke, N. & Chafetz, H. (2012) Criteria for distinguishing microbial mats and earths. *Society of Economic Paleontologists and Mineralogists Special Paper*, 101, 136–152.
<https://doi.org/10.2110/sepmsp.101.139>
- Sagemann, J., Bale, S.J., Briggs, D.E.G. & Parkes, R.J. (1999) Controls on the formation of authigenic minerals in association with decaying organic matter: an experimental approach. *Geochimica et cosmochimica Acta*, 63, 1083–1095.
[https://doi.org/10.1016/S0016-7037\(99\)00087-3](https://doi.org/10.1016/S0016-7037(99)00087-3)
- Saporta, G. de (1889) *Dernières adjonctions à la “Flore fossile d’Aix-en-Provence”, précédées de “Notions stratigraphiques et paléontologiques appliquées à l’étude du gisement des plantes fossiles d’Aix-en-Provence.”* G. Masson, Paris, France, 192 pp.
- Schieber, J. (1998) Possible indicators of microbial mat deposits in shales and sandstones: examples from the Mid-Proterozoic Belt Supergroup, Montana, USA. *Sedimentary geology*, 120, 105–124.
[https://doi.org/10.1016/S0037-0738\(98\)00029-3](https://doi.org/10.1016/S0037-0738(98)00029-3)
- Seilacher, A. (1970) Begriff und Bedeutung der Fossil-Lagerstätten. *Neues Jahrbuch für Geologie und Paläontologie*, 34–39.
- Selden, P.A. (2001) Eocene spiders from the Isle of Wight with preserved respiratory structures. *Palaentology*, 44, 695–729.
<https://doi.org/10.1111/1475-4983.00199>
- Selden, P.A., da Costa Casado, F. & Vianna Mesquita, M. (2006) Mygalomorph spiders (Araneae: Dipluridae) from the Lower Cretaceous Crato Lagerstätte, Araripe Basin, north-east Brazil: Cretaceous spiders from Crato, Brazil. *Palaentology*, 49, 817–826.
<https://doi.org/10.1111/j.1475-4983.2006.00561.x>
- Smith, D.M. (2012) Exceptional preservation of insects in lacustrine environments. *Palaaios*, 27, 346–353.
<https://doi.org/10.2110/palo.2011.p11-107r>
- Stolz, J.F. (2000) Structure of microbial mats and biofilms. *In*: R. E. Riding & S. M. Awramik (Eds), *microbial sediments*. Springer Berlin Heidelberg, Berlin, Heidelberg, pp. 1–8.
https://doi.org/10.1007/978-3-662-04036-2_1
- Street-Perrott, F.A. & Harrison, S.P. (1985) Lake levels and climate reconstruction. *In*: Hecht, A.D. (Ed.), *Palaeoclimate analysis and modelling*. John Wiley & Sons, New York, pp. 291–331.
- Suosaari, E.P., Reid, R.P., Playford, P.E., Foster, J.S., Stolz, J.F., Casaburi, G., Hagan, P.D., Chirayath, V., Macintyre, I.G., Planavsky, N.J. & Eberli, G.P. (2016) New multi-scale perspectives on the stromatolites of Shark Bay, Western Australia. *Scientific reports*, 6 (1), 1–13.
<https://doi.org/10.1038/srep20557>
- Varejão, F.G., Warren, L.V., Simões, M.G., Fürsich, F.T., Matos, S.A. & Assine, M.L. (2019) Exceptional preservation of soft tissues by microbial entombment: insights into the taphonomy of the Crato Konservat-Lagerstätte. *Palaaios*, 34, 331–348.
<https://doi.org/10.2110/palo.2019.041>
- Warren, L.V., Varejão, F.G., Quaglio, F., Simões, M.G., Fürsich, F.T., Poiré, D.G., Catto, B. & Assine, M.L. (2016) Stromatolites from the Aptian Crato Formation, a hypersaline lake system in the Araripe Basin, northeastern Brazil. *Facies*, 63, 1–19.
<https://doi.org/10.1007/s10347-016-0484-6>
- Wei, S.P., Cui, H.P., Jiang, Z.L., Liu, H., He, H. & Fang, N.Q. (2015) Biomineralization processes of calcite induced by bacteria isolated from marine sediments. *Brazilian Journal of Microbiology*, 46, 455–464.
<https://doi.org/10.1590/S1517-838246220140533>
- Wilby, P.R., Briggs, D.E.G., Bernier, P. & Gaillard, C. (1996) Role of microbial mats in the fossilization of soft tissues. *Geology*, 24, 787–790.
[https://doi.org/10.1130/0091-7613\(1996\)024<0787:ROMMIT>2.3.CO;2](https://doi.org/10.1130/0091-7613(1996)024<0787:ROMMIT>2.3.CO;2)